Biomimetic apatites functionalized with antioxidant phytotherapeutics: The case of chlorogenic and sinapic phenolic compounds

Omar Baklouti, Olivier Marsan, Fabrice Salles, Jalloul Bouajila, Hafed El-Feki, Christophe Drouet

MTLA 38 (2024) 102271

Contents lists available at ScienceDirect

Materialia

journal homepage: www.elsevier.com/locate/mtla

Full Length Article

Biomimetic apatites functionalized with antioxidant phytotherapeutics: The case of chlorogenic and sinapic phenolic compounds

Omar Baklouti [a,b], Olivier Marsan [b], Fabrice Salles [c], Jalloul Bouajila [d,*], Hafed El-Feki [a,1,*], Christophe Drouet [b,2,*]

[a] Laboratoire des Sciences des Matériaux et de l'Environnement, MesLab, University of Sfax, Tunisia
[b] CIRIMAT, CNRS, UT3, Toulouse INP, Université de Toulouse, France
[c] ICGM, Université de Montpellier, ENSCM, CNRS, France
[d] LGC, CNRS, UT3, Toulouse INP, Université de Toulouse, France

ARTICLE INFO

Keywords:
Biomimetic apatite
Polyphenol
Organic-inorganic hybrids
Phytotherapeutics
Antioxidant properties

ABSTRACT

Synthetic bone-like apatites (i.e. biomimetic apatites) increasingly attract attention in the field of bone substitutes due to their similarity to natural bone mineral and their intrinsic surface reactivity, as opposed to conventional hydroxyapatite. Associations with a range of bioactive species can be a way to further tailor their properties after implantation. In the present work, we have focused on the preparation of hybrid materials combining biomimetic apatites, doped or not with antibacterial Ag^{+} ions for added antimicrobial pertinence, and two biophenolic compounds, namely chlorogenic acid (CA) and sinapic acid (SA). Using complementary characterization techniques, especially FTIR and Raman spectroscopies, as well as Monte Carlo computational simulations, we elucidate the possible interaction between such biophenolic molecules and apatite. The follow-up of isotherms of adsorption also pointed out the quantitative sorption of CA and SA onto biomimetic apatites, potentially up to larger extents than reported so far in the literature for apatitic substrates. Finally, antioxidant properties of prepared hybrids were measured via free radical scavenging tests using DPPH as reactant, showing that the studied phytotherapeutic agents retained antioxidant properties after the adsorption process. This work thus evidences that bone-like apatites can be quantitatively associated to biophenolic bioactive agents to further modulate their properties as smart bone substitutes, providing them additional antioxidant features, among others.

1. Introduction

Plant-derived bioactive agents are increasingly appealing in the biomedical field to confer various functionalities to biomaterials and medical devices. Indeed, so-called "phytotherapeutic agents" may exert a variety of properties such as antimicrobial, antioxidant, anti-inflammatory, anticancer, among others. Beyond this multi-functionality, one of their particular appeals obviously arises from their presence in Nature, conferring to these compounds a bio-sourced character, as opposed to common drugs such as antibiotics and most chemotherapeutics.

Among such phytotherapeutic agents, phenolic acids and their derivatives occupy a particular position due to their relatively high abundance in various plants, as secondary metabolites, and to their reported bioactivity, for instance to promote/restore cardiovascular, gastrointestinal and liver functions [1]. In plants, they have a protective effect against both biotic (via bacteria, fungi, nematodes, insects, etc.) and abiotic stress (moisture, temperature, injury, presence of heavy metals, etc.). The chemical composition of phenolic compounds involves aromatic cycle(s) and hydroxyl groups (–OH), leading to particular reactivity through the presence of several conjugated C=C double bonds. This also implies the side-chain(s) providing additional stabilization of the phenol ring and promotion of antioxidant activity [2] as in hydroxycinnamic acids. This structure indeed favors the release and capture of hydrogen atoms. The antioxidant activity of phenolic compounds has been related to the number of OH groups in the following

* Corresponding authors.
E-mail addresses: jalloul.bouajila@univ-tlse3.fr (J. Bouajila), hafed.elfeki@fss.usf.tn (H. El-Feki), christophe.drouet@cirimat.fr (C. Drouet).
[1] https://www.researchgate.net/profile/Hafed-Elfeki
[2] https://www.christophedrouet.com/highlights.html

https://doi.org/10.1016/j.mtla.2024.102271
Received 15 July 2024; Accepted 21 October 2024
Available online 30 October 2024

order: tri-hydroxy phenolic acids >di-hydroxy (catechol) >mono-hydroxy [2]. In the medical domain, these antioxidant properties were hypothesized to play a role in carcinogenesis, and polyphenols could have a proapoptotic effect on cancer cells via their pro-oxidizing action [3,4]. Indeed, the accumulation of free radicals in the body may cause harm to cells by interacting with DNA and proteins, and potentially leading to carcinogenesis.

Two main families of phenolic compounds can be identified, namely flavonoid and non-flavonoid ones [5]. Chlorogenic acid (CA) is a member of the non-flavonoid subfamily of such "biophenols", and is one of the most illustrious biophenol compounds. It is found in numerous plants such as vegetable, fruit, Urtica urens [6], herbs, etc. [7]. It is a lightly water-soluble ester formed from quinic and caffeic acids (i.e. the latter being a trans-cinnamic acid); it is thus a polyphenol bearing a catechol group (*ortho* di-hydroxyphenolic). It has been considered in a large amount of literature studies. CA was reported to exert many biological properties such as anti-oxidant [8] and anti-inflammatory [9–12], anticancer [13], antibacterial [14,15], antihypertensive [16] and anti-diabetic [17]. It was indeed shown to have positive activity on peripheric organs such as muscles (e.g. increased glucose consumption), liver (e.g. neoglycogenesis) and intestines (e.g. amylase inhibition) for glycemic control [18]. From the antimicrobial viewpoint, CA has been shown to exhibit various effects making it suitable as preservative food additive. Studies have for example pointed out bactericidal effects against *Staphylococcus aureus* [19], *Staphylococcus epidermidis* [20], *Escherichia coli* [21], *Helicobacter pylori* [22], *Stenotrophomonas maltophilia* [23] and *Klebsiella pneumonia* [24]. It was also reported to play an inhibitory role on multi-drug resistant bacteria [25] and their biofilm formation [26].

Although less studied in the literature, Sinapic acid (SA) is another appealing biophenol compound. It bears only one hydroxyl group attached to the aromatic cycle (mono-hydroxy) and derives from caffeic acid with however the presence of two methoxy groups ($-OCH_3$) replacing an –H and an –OH on the cycle. It was also reported to have various biological properties such as anticancer [27], antioxidant [28], antimicrobial [29], and anti-inflammatory [30–32], among others.

Despite the quite large interest of the general population and researchers for such (poly)phenolic agents derived from plants, their use was mainly considered as bioactive agents by themselves, but their combination with (bio)materials to generate functional composites/hybrids has been much less explored. Some examples have been reported, like the coating of gelatin with CA for the preservation of seafood [33], chitosan/polycaprolactone (PCL) nanofibers with CA-loaded halloysite nanotube or CA-encapsulation in Pickering emulsion-stabilized by chitosan nanoparticles for food packaging [34,35]. Much fewer reports seem to be available in the domain of implantable devices as in bone regeneration. Yet, the field of orthopedics and maxillofacial surgeries could benefit from the multifunctional character of biophenols such as CA or SA, among others, for example to convey antimicrobial or anti-inflammatory properties, but also through their powerful antioxidant features, which can be exploited to fight against oxidative stress of cells/tissues, related to aging and diseases like cancer.

In the context of bone applications, few reported seem to be available. We can cite for example polyphenol-enriched silica and bioglasses, eventually combined to a polymer like polycaprolactone (PCL) [1,36,37]. The combination of biophenolic compounds with calcium phosphates has seldom been mentioned in the literature. Some studies have dealt with the preparation of hybrid polyphenol/hydroxyapatite nanoparticles [5] or to prepare a CA-loaded CaP (supposedly apatite-like)/chitosan nanogel [38], although bone applications were not specified and the intended usage seemed to be more oriented toward nanomedicine. One of these works examined the interaction between several polyphenols (including chlorogenic acid) and hydroxyapatite (HA) nanoparticles, either through synthesis in their presence in the precipitating medium or via subsequent adsorption. The first approach generally led to an inhibition of CaP crystallization, and the adsorption pathway seems to be more relevant. However, a limited amount of polyphenol was detected on the HA particles prepared in that study, involving a drying stage at 100°C prone to favor HA crystallinity and thus limit its surface reactivity.

In this context, the present work aimed at exploring the possibility to prepare hybrid biomaterials based on (poly)phenolic compounds, namely CA and SA, and biomimetic apatites analogous to bone mineral and exhibiting a significantly higher surface reactivity than conventional, well-crystallized hydroxyapatite [39,40]. Indeed, biomimetic apatites mimic the chemical composition and crystalline structure of natural bone apatite. In contrast to regular hydroxyapatite, which is stoichiometric and does not exhibit a high surface reactivity, biomimetic apatites exhibit an ionic and hydrated layer on the surface of the nanocrystals – as in bone mineral – which contains highly labile ions that can take part easily in ion exchange and molecular adsorption/release processes. Thus, considering biomimetic apatites as carrier of (poly)phenolic molecules appears as a smart way to develop novel implants, highly bioinspired both from their (poly)phenolic content and nature of apatite, to allow faster bone regeneration.

The mode of interaction between these bio-organic molecules and the apatite nanocrystals surface will be scrutinized by complementary experimental (FTIR, Raman microscopy) and molecular simulation approaches, to shed light on the probable interaction mechanisms at play. The possibility to co-functionalize the apatite nanocrystals with bioactive ions, namely Ag^+, will also be investigated, as this would allow fabricating for the first time some codoped Ag/(poly)phenol/bone-like apatite biomaterials of relevance to clinical application – typically to aim the treatment or prevention of infections in bone sites, taking into account the added antimicrobial properties of Ag^+. Finally, the capacity for such phytotherapeutic agents to retain their antioxidant properties after the sorption process onto biomimetic apatite will be verified. This study thus intends to demonstrate the possibility to prepare highly nature-inspired biomaterials, by associating plant-derived phenolic compounds with bone-like "biomimetic" apatites in view of the development of bone scaffolds with oxidative stress control ability.

2. Materials and methods

2.1. Reagents

The following reagents have been used throughout the experiments: diammonium hydrogen phosphate ($(NH_4)_2HPO_4$, ACS, M = 132.05 g/mol, Lot A1015407 628), calcium nitrate tetrahydrate ($Ca(NO_3)_2{\cdot}4H_2O$, ACS, M = 236.15 g/mol, Lot AM1339021 840), and sodium hydroxide (NaOH, ISO, M = 40.00 g/mol, Lot B1289298 624) were purchased from Emsure® (Darmstadt, Germany). Potassium bromide (KBr for IR spectroscopy, Uvasol®) was purchased from Merck, Darmstadt, Germany. Chlorogenic acid (CA) and Sinapic acid (SA), 98% purity, were purchased from Apollo scientific and Acros Organics (India).

2.2. Biomimetic apatite synthesis

The biomimetic apatite sample used as adsorption substrate in this work was prepared at room temperature and physiological pH by precipitation through the mixing of two solutions. The first solution contained calcium nitrate tetrahydrate $Ca(NO_3)_2 \cdot 4H_2O$ solution (52.2 g in 750 ml of deionized water) as calcium source and the second solution contained diammonium hydrogenphosphate $(NH_4)_2HPO_4$ (120 g in 1500 ml of deionized water) as phosphate source. The calcium solution was rapidly added into the phosphate solution. The use of an excess of phosphate ions allowed us to buffer the pH close to the physiological value (around 7.4) without the use for an external additive such as TRIS which was also adsorb onto the apatite nanocrystals in formation and modify their surface reactivity. The precipitating medium was left then to maturation for one day at room temperature (leading to the sample denoted hap1d) and was then filtered on a Buchner funnel, washed

immediately with deionized water, freeze dried and stored in a freezer to avoid any alterations of the nanocrystalline apatite prior to use. After unfreezing, this sample was used for the adsorption study.

A silver-loaded apatite analog was also used. It was prepared by the same method, but in the presence of 2 mol.% of silver nitrate ($AgNO_3$, Alfa Aesar, Erlenbachweg, Kandel, Germany) replacing the same amount of calcium nitrate in the first solution. This silver-doped sample will be denoted hap1d-Ag.

2.3. Physicochemical characterization

The crystalline structure of the calcium phosphate adsorbents was checked by X-ray powder diffraction (XRD). The analyses were carried out on monochromatic Bruker D8 diffractometer using the Cu Kα radiation (λ= 1.5418 Å).The samples were scanned in the 2θ range from 20 to 60° with a step size of 0.02° and a counting time of 1 s per step.

The nature of the CaP phase was confirmed by Fourier-Transform Infrared Spectroscopy (FTIR) in transmission mode using the KBr pellet technique, on a Nicolet IS50 spectrometer (Thermo Scientific, Waltham, MA, USA) in the 400-4000 cm^{-1} wavenumber range and a at a resolution of 4 cm^{-1}.

Raman analyses of the samples were carried out before and after adsorption using a confocal Labram HR800 micro-spectrometer (Horiba FRANCE SAS, Palaiseau, France). The samples were exposed to an Ar-diode laser (λ = 532 nm) with a power of 10.2 mW. An uncertainty on Raman shifts lower than 1 cm^{-1} has been confirmed using a silicon calibration standard at 520.7 cm^{-1}. An optical objective ×100 was used for all analyses.

2.4. Chlorogenic acid (CA) and sinapic acid (SA) sorption

Chlorogenic (CA) and sinapic (SA) acids were used as starting adsorbates in this work. Their respective chemical formula is given in Fig. 1.

CA and SA adsorption was realized in deionized water containing dissolved KCl (10^{-2} M) to provide a relatively stable ionic strength during the tests, and at room temperature (22°C). For each datapoint, 5 ml of solution of CA or SA was contacted with 20 mg of apatite substrate. Preliminary solubilization trials of the two acids showed the limited solubility in water; for SA, experiments were carried out in a water: ethanol 50/50 medium to promote its dissolution and provide a more stable environment than pure water for this metastable molecule. Due to the potential sensitivity of the two molecules to light, the experiments were carried out in aluminum foil-covered vials.

CA and SA concentrations were followed (in the range 0-5 g/L for CA and 0-10 g/L for SA). The natural pH values of such solutions indicated that the medium was indeed acid (pH between 3.5 and 5.5) whereas the adsorption is favored in the pH close to that physiological. Thus, the stock solutions prepared in KCl 10^{-2} M/deionized water underwent a treatment by adding drops of diluted solutions of NaOH/HCl allowing us to set the pH values close to 7.5 for the starting solutions.

After 1 h of contact time between the adsorbate and the biomimetic apatite sample, the amount of CA or SA remaining in solution was determined by titration of the supernatants, after syringe filtration (0.45 μm membrane cutoff), by UV spectrophotometry (Shimadzu 1800, Kyoto, Japan). To this aim, the optical density at λ = 329 nm for chlorogenic acid and at 305 nm for sinapic acid (absorption maximum) was monitored. This contact time and other conditions were selected on the basis of the results of preliminary experiments, typically to determine the amount of time sufficient to reach thermodynamic sorption equilibrium. After the corresponding time interval, the suspensions were sampled through direct filtration using 0.45 μm membrane filter. The amount of CA or SA adsorbed (Q_{ads}) was then calculated by difference between the initial adsorbate concentration (C_i) and the final concentration (C_f) in the supernatant, and given per gram of apatitic adsorbent using the following equation:

$$Q_{ads} = (C_i - C_f) \times V/m_{ap} \quad (1)$$

where V is the total volume of initial solution and m_{ap} the mass of apatite substrate used.

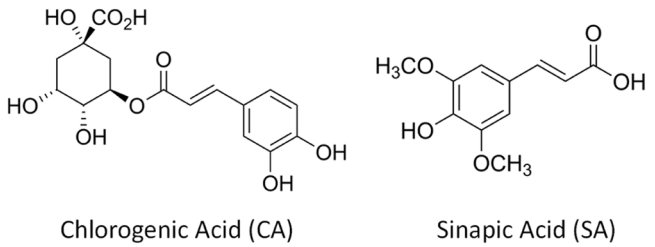

Fig. 1. Chemical formula of chlorogenic acid (CA) and sinapic acid (SA).

2.5. Computational modeling of CA and SA sorption

In order to investigate the plausible interaction existing between the apatitic substrate and the CA or SA molecules, Monte Carlo simulations were performed using SORPTION (Materials Studio by BIOVIA, Dassault, San Diego, 2020). Indeed, using Monte Carlo simulations, it is then possible to extract the adsorption enthalpy and plausible configurations for molecules or ions at the surface of the solids.

Before that, preliminary DFT calculations have been performed to extract partial charges using $DMol^3$ (BIOVIA) for neutral CA and SA molecules. In this case, a geometry optimization procedure was performed on the two molecules using the density functional GGA PBE and considering polarization functions for hydrogen atoms (DNP) and taking into account all electrons. The convergence of the calculations was reached when energy, maximal force and maximal displacement variations were lower than 10^{-5} Ha, 0.002 Ha/Å and 0.005 Å respectively. The corresponding partial charges for SA and CA are given in Fig. 2.

Regarding the solid, the hydroxyapatite (HA) structure was built from the data available in the literature [41]. After a DFT geometry optimization with $DMol^3$ using the same parameters than for molecules, the structure was used to build (001) slab with a vacuum of 20Å and a unit cell extended to 4×4×1 multi-cell to reach parameters a = 37.68 Å; b = 27.52 Å; c = 38.13 Å and angles equal to 90°. From this slab, the pending bonds was finished by OH groups and the partial charges were then calculated using Mulliken equalization method (available in Materials Studio as qEq method). The structure was thus reoptimized using Forcite with the so-obtained partial charges and UFF force field for the electrostatic and van der Waals contributions of energy respectively. For the classical geometry optimization, the Ewald summation method was used for the electrostatic calculations in the multi-cell while the Van der Waals interaction between atoms was calculated using a cut-off of 12.5 Å.

Using this slab and the optimized SA and CA molecules, it was then possible to perform Monte Carlo calculations. Again Ewald summation for electrostatic interactions and an atom-based cut-off of 12.5 Å were used to calculate and minimize the energy of the system, through partial charges previously obtained and UFF force field for the Lennard-Jones parameters for both solid and molecules. The Monte Carlo simulations were performed at 300K following the procedure including 30 millions of steps for equilibration and 5 millions of steps for production.

In the case where water was considered as solvent, we used TIP4P-2005 force field [42].

Different Monte Carlo calculations were performed to identify the potential adsorption sites existing on the HA surfaces: one calculation with 1 or 3 CA or SA molecules without solvent and 1 or 3 CA or SA molecules with 50 H_2O to investigate the effect of possible interactions between molecules or between molecules and solvent. It followed from the calculations that no interactions between molecules were observed.

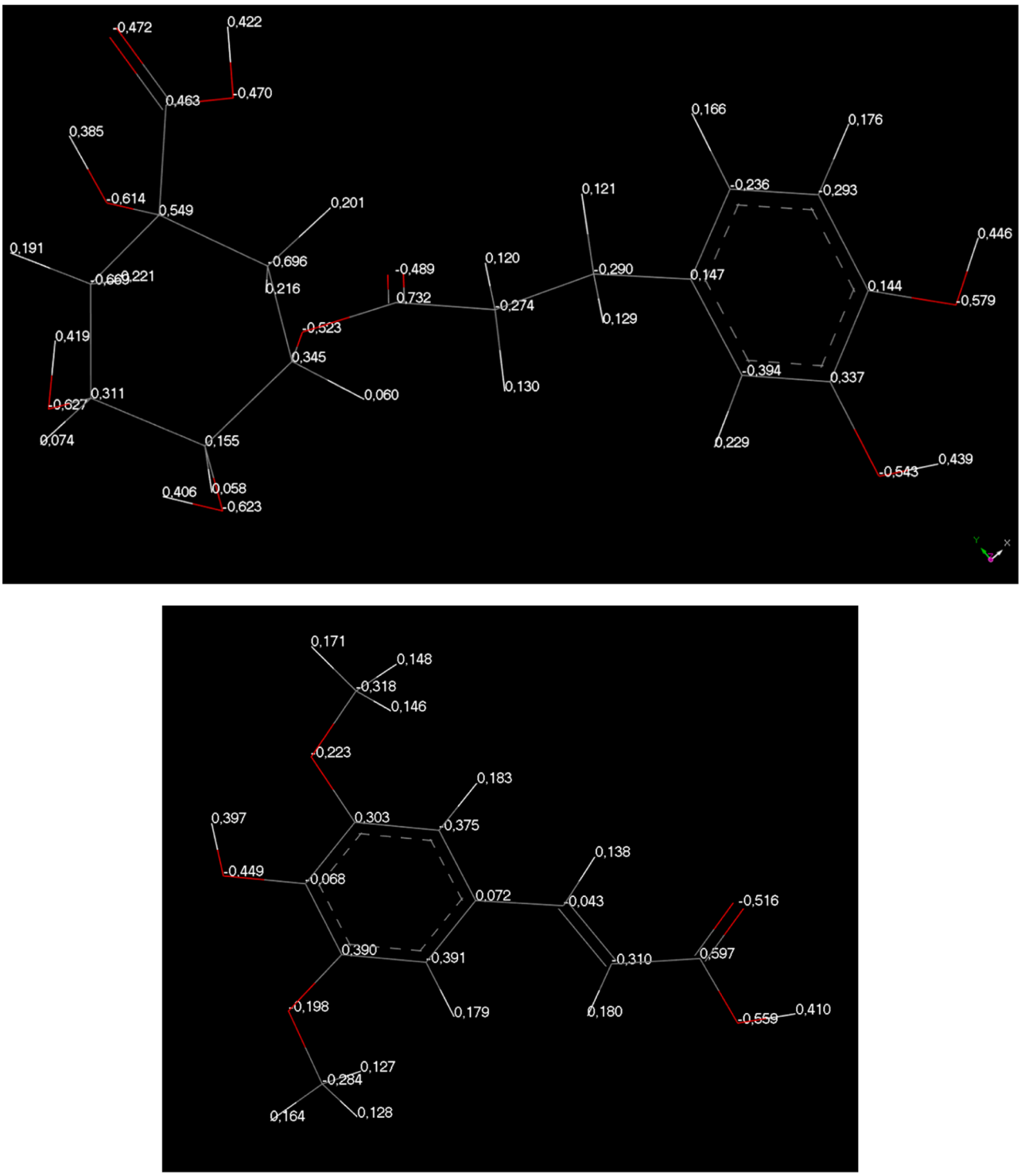

Fig. 2. Partial charges for chlorogenic acid (CA, top figure) and sinapic acid (SA, bottom figure) extracted from DFT calculations (the atoms C, H, O are respectively represented in grey, white and red).

2.6. Follow-up of antioxidant properties

The free radical scavenging activity of CA or SA, either alone or in combination to the apatite sorbent, was assessed using the diphenyl-2-picryl hydrazyl (DPPH) reagent (Sigma Aldrich), thus measuring their related antioxidant activity. The method described by Saoudi et al. [43] was used to quantify this free radical scavenging capacity. In a typical experiment, 1 mg of sample was introduced in 1 ml DMSO (Sigma Aldrich). A dilution by a factor 2 was then undergone, and 20 μL was taken and added to 180 μL of DPPH solution in methanol (3.5 mg in 7.5 ml then diluted by 10) or in pure methanol (Sigma Aldrich) for the control "blank" measurement, reaching a final concentration of 50 mg/L. The mixture was homogenized and incubated for 25 min in the dark at room temperature, followed by measurement of the absorbance of all samples at $\lambda = 524$ nm. Finally, the percentage of inhibition of free radical scavenging activity for each sample was calculated using the equation:

$$\%\ inhibition = \frac{A_{blank} - A_{sample}}{A_{blank}} \times 100 \quad (2)$$

where A_{blank} is the absorbance of the negative control reaction without any active compound, and A_{sample} is the absorbance of the tested sample.

The evaluation of this activity was then expressed as IC_{50} (μg/mL), indicating the concentration of the test product required to bring about a 50% reduction in the initial DPPH concentration. In the case of the hybrid materials, the IC_{50} value reported in this study refer to the actually adsorbed amount of phenolic compound estimated from the adsorption isotherms, thus leading to IC_{50} values in μg of phenolic compound per milliliter. All measurements were carried out in triplicate, with ascorbic acid (vitamin C) as reference.

3. Results and discussion

3.1. Preparation of the biomimetic apatite-based adsorbents

The CaP substrate used in this work for the preparation of the biophenol/CaP hybrids proved to exhibit an apatitic structure as confirmed by XRD, despite a rather low crystallinity degree typical for biomimetic nanocrystalline apatites analogous to bone mineral (Fig. 3a). These results are identical to those obtained previously by some of us and well documented in the literature [44,45].

Application of Scherrer's formula to the characteristic (002) and (310) diffraction peaks allowed us to evaluate, in a first approximation, the mean crystallite dimensions, reaching *ca.* 39 nm in length and *ca.* 7 nm in width/thickness, thus confirming the expected nanocrystalline character of the sample precipitated in close to physiological conditions (low temperature (RT), pH buffered close to 7.4, no heat drying). The low crystallinity of the biomimetic 1-day matured sample prepared does not allow for a much more detailed analysis of the XRD features as reported previously [45]. Therefore, vibrational spectroscopies such as FTIR or Raman appear as particularly helpful to convey additional/complementary information on the local chemical environment of phosphate and to some extent OH^- ions from the apatite specimen [45]. Fig. 3b reports the FTIR spectra of the precipitated apatite powder. As expected, they display the typical vibrational signature of bone-like apatite. In particular, we can remark the low intensity of the apatitic OH bands at 3563 and 633 cm^{-1}, and the presence of a clear shoulder around 533-534 cm^{-1} on the $\nu_4(PO_4)$ domain in FTIR, which is characteristic of non-apatitic HPO_4^{2-} ions from the amorphous surface layer on bone-like apatite nanocrystals. Both the low intensity of OH band and the presence of HPO_4^{2-} clearly show the nonstoichiometric character of the precipitated apatite, and the presence of non-apatitic HPO_4^{2-} also demonstrates that the sample is indeed biomimetic to bone mineral (in contrast to well-crystallized, stoichiometric HA which do not show these features). For information, a typical FTIR spectrum for a natural bone sample and stoichiometric HA are provided as additional resource as **Fig. S1** in the Supporting Information.

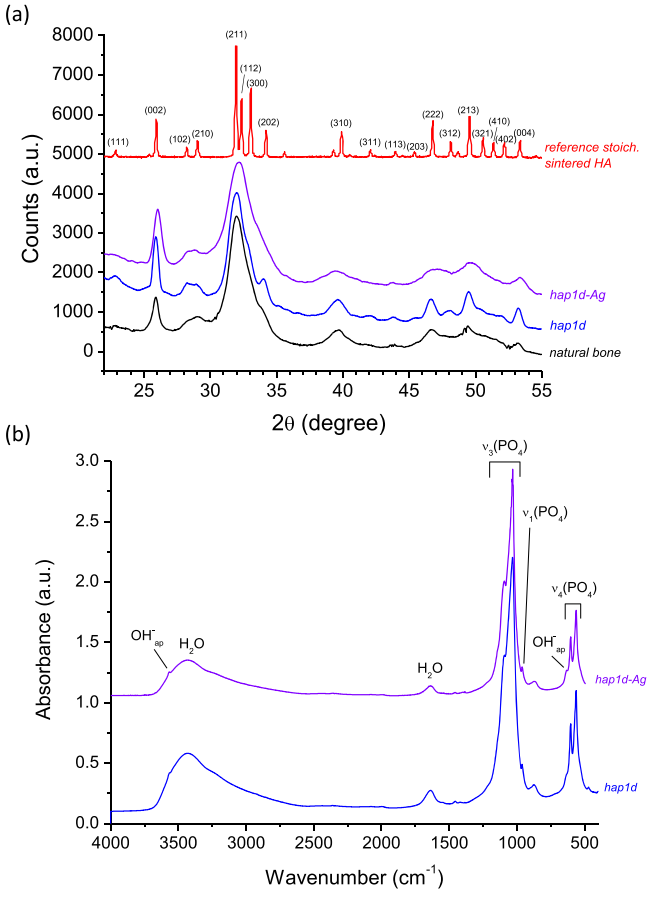

Fig. 3. (a) XRD patterns for the apatitic substrates (raw or Ag-doped) used in this work, as well as a stoichiometric hydroxyapatite reference and a natural bone sample (rat bone, 9 months old, CIRIMAT internal collection) ; (b) FTIR spectra for the same raw and Ag-doped substrates.

An Ag-containing apatitic substrate was also investigated in this work as second possible substrate. Ag^+ doping (expectedly by replacing some Ca^{2+} ions and changing accordingly the HPO_4^{2-}/PO_4^{3-} speciation and/or OH^- contents for retaining the overall electroneutrality) was indeed undergone to provide additional properties, such as antimicrobial, to the hybrid biomaterials studied. The final Ag^+ content was titrated by AAS to reach 0.11 mol per apatite unit formula. This Ag-doped sample was found to essentially lead to very similar XRD and FTIR features, without detectable traces of secondary phases, as may be expected from such low doping rates, and as verified on Fig. 3a,b. This sample was previously analyzed in more details in another study [46]. Again, bone-like features such as nanosized crystal dimensions, non-stoichiometry and presence of a non-apatitic surface layer can be highlighted for this silver-doped apatite compound.

3.2. Preparation of the biophenol/biomimetic apatite hybrids via adsorption

The preparation of hybrid biophenol/biomimetic apatite powders – usable as biomaterials precursors – was then explored using an adsorption process. In a first illustrative case, we explored the interaction between chlorogenic acid (CA) and the biomimetic (undoped) apatite sample mentioned above. An adsorption protocol was used, putting in contact the two components at RT, close to physiological pH (7.5), and in KCl 10^{-2} M to ensure a rather stable and sufficient ionic strength in the medium for avoiding artifactual limitation of ion diffusion during the sorption process.

In a first stage, a kinetic study was undergone to determine the amount of time needed to reach thermodynamic equilibrium for each adsorption datapoint. To this aim, different contact times from 0 to 100 min were tested to reach minimum time for equilibration of the system. The kinetics of adsorption of CA was followed by UV-vis spectrophotometry, analyzing the supernatants and comparing to the initial concentration. The obtained kinetic curve plotted the evolution of the calculated absorbed amount Q_{ads} vs. the equilibrium time using an initial concentration in CA of 0.2 g/L. According to the UV-vis data, in our working conditions, the absorbance and thus CA adsorption reached quasi-equilibrium in about 30 min. For security, a 1-hour contact time was thus selected for all the rest of the study.

In a second step, we thus aimed at determining the isotherm of adsorption of CA on 1-day mature biomimetic apatite. This was achieved by similarly following the amount adsorbed as a function of the equilibrium CA concentration (C_{eq}). Initial concentrations of CA from 0 to 5 g/L were investigated (leading to equilibrated concentrations in the

range 0-3 g/L). The related plotted isotherm (at RT) is reported in Fig. 4a.

As can be expected, the value of Q_{ads} was found to increase with C_{eq}, with a tendency to progressively stabilize toward high C_{eq} values. For example, for an initial concentration of $C_i = 5$ g/L, the equilibrated concentration reached $C_f = C_{eq} = 2.573$ g/L, which corresponds to the nearly stabilized value of 0.58(4) $g_{CA}/g_{apatite}$ (corresponding to 1.65 mmol CA/g apatite). The obtained isotherm can be tentatively fitted to usual mathematical isotherm models relevant to apatitic compounds (see for example [47]). Fitting to the Freundlich model, described by the equation $Q_{ads} = k_F . C_{eq}^{1/n}$ led to a correlation coefficient $R^2 = 0.9644$ (and a value of $n \cong 1.41$). Interestingly, fitting to the Sips model – also known as Langmuir-Freundlich – led to an even better match, with a correlation coefficient $R^2 = 0.9821$. This value, close to unity, shows that the adsorption of chlorogenic acid onto biomimetic apatite can be rather satisfactorily fitted with the Sips model. As explained in details elsewhere [47,48], this model is typically obtained to depict the sorption of a molecule with different interacting end-groups and/or the heterogeneity of the adsorbent that can expose various types of surface sites (thus associated to different heats of adsorption). The Sips isotherm can be described from a variation of the Langmuir "idealized" model by the equation:

$$Q_{ads,e} = Q_m \times \frac{K_S \times {C_{eq}}^m}{1 + K_S \times {C_{eq}}^m} \quad (3)$$

While in the ideal Langmuir case, $m = 1$, the exponential Sips parameter m was found here to reach $n \cong 1.39$. This difference from unity thus shows the departure from the theoretical hypotheses of Langmuir which stipulates similar heats of adsorption for all adsorption sites and the absence of interaction between adsorbed species. In the present case, the value of m differs significantly from one, as was also previously found for other organic molecules on bone-like apatitic surfaces [48]. A value of m greater than unity is usually informative of a positive cooperativity among the adsorbing molecules, suggesting here that adjacent CA molecules may support each other's sorption to the apatite surface.

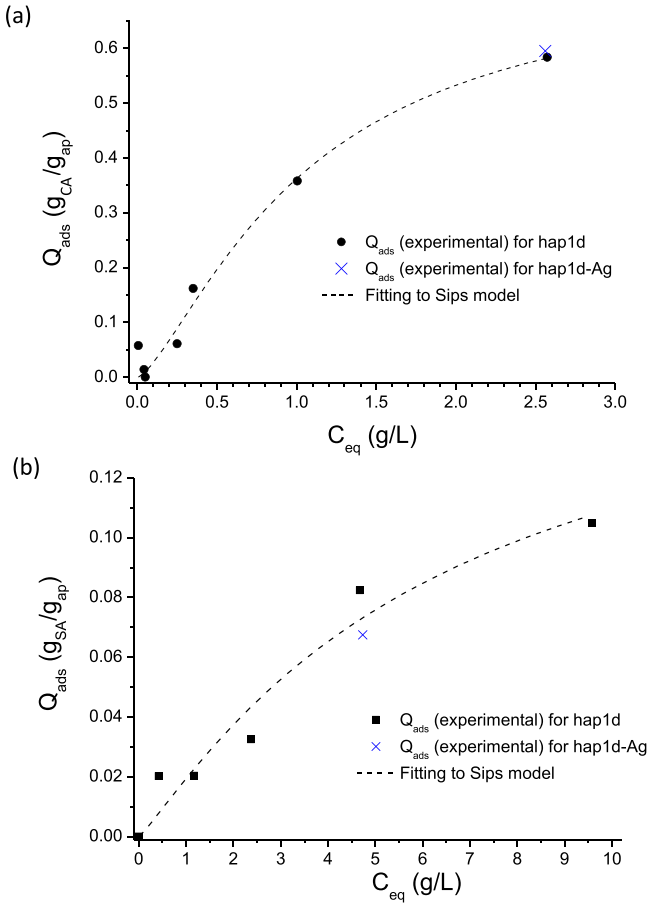

Fig. 4. Adsorption isotherms, at RT and pH ~7.5 (in KCl 10^{-2} M), for CA (a) and SA (b) on undoped and Ag-doped nanocrystalline apatites matured 1 day.

It may be noted that the adsorbed amount of CA measured on the Ag-doped sample for the maximal initial concentration of CA at 5 g/L led to a value very close to the one obtained for the undoped hap1d sample (see Fig. 4a). These findings thus allow widening the perspectives of use of (poly)phenol-doped biomimetic apatites to ion-functionalized apatites so as to convey additional properties that may prove to be synergistic or complementary. Here, we illustrate this with the Ag^+ ion that is well known to exhibit a variety of biofunctionalities such as antibacterial and antifungal.

The above results thus show that biophenolic compounds such as chlorogenic acid can be adsorbed quantitatively, and following a Sips isotherm model, onto biomimetic apatites eventually doped with functional ions.

In order to widen further this concept to other biophenols, we have also carried out experiments using sinapic acid (SA) as adsorbate. As mentioned in the Introduction section, while CA is a polyphenol bearing a catechol group, SA is monophenolic compound bearing two methoxy groups. Although SA is also associated to various functional properties of relevance to biomedicine, and thus promising for medical use as in bone substitutes, this molecule appears more delicate to manipulate due to its lower water solubility. It has for example been reported that CA has a greater stability in water than SA, and several factors such as temperature, pH and light may affect its behavior. A first series of experiments was carried out in water, but leading to dissolution limitations and a relative instability of the solution. Therefore, the SA adsorption experiments were run in water:ethanol mixture 50:50. Beside the favored dissolution of SA, the presence of ethanol may also help stabilizing the solution by limiting undesirable molecular interactions.

Considering that the SA molecule has not been altered during the tests (and taking comparative conditions for the preparation of the standards), the adsorption isotherm (still at physiological pH and RT) obtained for SA in these conditions is reported in Fig. 4b. The shape of the isotherm in the 1-10 g/L initial concentration range appears rather close to the case of CA, with a progressive increase and start of stabilization of Q_{ads} upon increasing SA concentration. If the experimental datapoints are once again fitted to a Sips model, the mathematical fit leads to a value of m of 1.12. As for CA, this exponent is greater than one (although in a less marked manner) and thus suggests again the possible existence of positive cooperativity among adsorbing SA molecules. It may however be remarked that, for a similar value of C_{eq} of for example 2.5 g/L, the amount of adsorbed SA (*ca.* 0.03-0.04 g/g apatite, corresponding to 0.13-0.18 mmol SA/g apatite) is noticeably lower than CA (*ca.* 0.58 g/g apatite, corresponding to 1.65 mmol CA/g apatite). Although SA sorption was followed here in water:ethanol environment compared to pure water for CA, these results suggest that chlorogenic acid can be significantly more retained by the biomimetic apatite surface compared to SA (of a factor close to ×10). This could be related to the presence of fewer –OH groups in the SA molecule and the steric hindrance of the two methoxy groups. To our knowledge, these are the first reported data for a comparison of the sorptive behavior of chlorogenic and sinapic acids on an apatitic adsorbent. Also, it may be pointed out that the adsorbed amount of CA measured here are about 20 times larger than those reported by Palierse et al. [49] on a non-biomimetic apatite substrate. The bone-like character (and related surface reactivity) of such biomimetic apatites thus appears particularly relevant for increasing the potential dose of CA or related polyphenols on apatites while achieving this combination by a controlled adsorption process.

As previously for CA, it may be noted here that the Q_{ads} value found for SA on the Ag-doped sample (for an initial concentration of 5 g/L) is

again close to the value found without silver doping. Thus, for a given adsorbate among CA or SA, the Ag-doped and undoped samples seem to be associated with similar adsorbed amounts. These compounds (corresponding to an initial concentration of 5 g/L) will be further studied in the evaluation of the antioxidant properties later in this study.

3.3. Insight on desorption

In our working conditions, it was interesting to evaluate the relative amount of adsorbed CA and SA, respectively, that could be released passively from the surface of hap1d upon immersion on physiological serum, namely a solution of NaCl 0.9%, at RT and over a duration of 48 h. These tests were realized (200 mg soaked in 5 mL) starting from apatite samples loaded with CA or SA, starting from an initial concentration of 5 g/L. Our quantitative results showed that 3% and 20% of adsorbed CA and SA were released, respectively, upon immersion in the NaCl solution. These findings thus suggest that the majority of the biophenolic molecules remained in an adsorbed state after aqueous immersion. While these observation could appear surprising at first, taking into account the absence of endgroups in the CA and SA composition know to exhibit a high affinity for the surface of apatite, these findings are of the same order of magnitude (only up to a few cumulated %) as those reported by Palierse et al. [5] for the desorption of chlorogenic acid or rosmarinic acid from an apatitic substrate.

3.4. Physicochemical characterization of hybrids – toward an understanding of the mode of interaction

The structure of the phosphocalcic adsorbents was cross-checked by XRD after adsorption of CA or SA (typically for an initial solution concentration of 5 g/L). As may be expected, the results (Fig. 5) confirm that the apatitic nature of these samples is preserved as no significant difference was noticed after CA or SA sorption on the apatitic signature by XRD, independently on the Ag doping. Thus, in all cases, the previously described characteristic features of bone-like biomimetic apatite were retained. However, traces of KCl (used in the adsorption medium to limit artifacts linked to a too low ionic strength hindering the natural diffusion of species) were punctually detected as remaining impurity. Also, some additional low-intensity lines could also be detected at 24.6, 27.6 and 37.3° for one of the samples (hap1d-Ag). Although the exact attribution of these lines could not be irrefutably made, some relationship with chlorophenyl derivatives could not be ruled out due to some vicinity with the pattern of chlorobenzoic acid PDF file #12-0905 (such a partial chloration may have been related to the acidification with HCl during pH control).

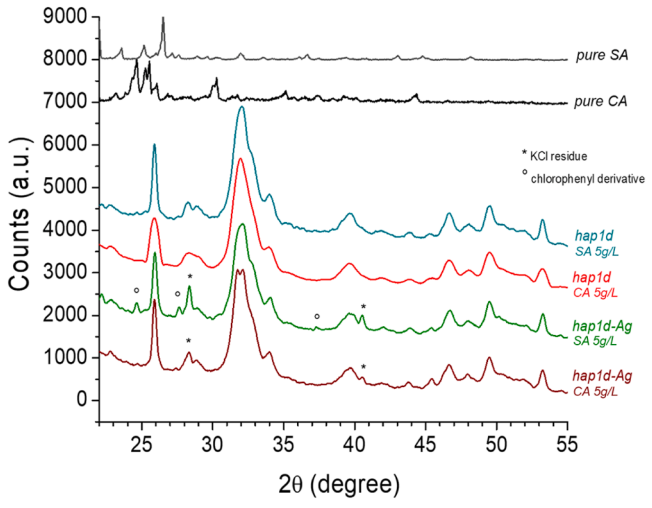

Fig. 5. XRD data on hybrids formed by CA or SA sorption on biomimetic apatite (matured 1 day), raw or Ag-doped.

Analyses by vibrational spectroscopies were also carried out to examine the hybrids. FTIR data (**Fig. S2** in Supporting Information) reports some characteristic spectra. Again, it may be seen that the physicochemical features of the apatite phase do not seem to be noticeably altered after CA or SA adsorption, and additional bands can be detected as the concentration of adsorbate in the medium increases. However, such additional bands are especially observed in the range 1200-1800 cm^{-1}. The pure chlorogenic acid molecule theoretically also exhibits IR bands relating to the OH groups stretching at 3338 and 3471 cm^{-1}, and to OH bending of the phenol function at 1382 cm^{-1}, but the presence of water associated to the biomimetic apatite phase make it difficult to detect these spectral contributions for the high frequencies contributions. The band assignable to the C=O stretching vibration of the carboxylic group is expected around 1729 cm^{-1}, whereas the band at 1684 cm^{-1} is due to the C=O stretching vibrations of the ester groups [50]. The stretching vibrations of the C=C fragment is expected at different Raman shifts, including at 1640 cm^{-1}, but again superimposed with the HOH bending of water, whereas the bands derived mainly from stretching vibrations of the aromatic ring are in the range 1500-1600 cm^{-1}. The band at 1443 cm^{-1}, attributed to a phenyl ring stretch, was previously assigned to the C3-O-H group [24]. The in-plane bending band of C-H in the aromatic hydrocarbon is expected at 1321 cm^{-1}, and out-of-plane bending bands are supposedly located [51] at 819 and 600 cm^{-1}but the latter are again bound to be superimposed with phosphate vibrations of the apatite phase. CH_2 stretching vibrations are expected to give rise to an absorption band [52] around 2956 cm^{-1} but it is hardly seen in our case, possibly also due to the rather limited amount of adsorbed molecule on the apatite crystal surface. The observation of weak bands at 1692, 1632, 1606, 1525, 1453, 1400, 1279, 813 and 767 cm^{-1} in the spectrum of hybrid samples, and more clearly for the CA concentration of 5g/L seem to confirm the adsorption event. In fact, these signals whose wavenumbers are displaced by 5 and 10 cm^{-1} with respect to those detected in pure CA are likely ascribable to phenyl ring stretching and phenol bending vibrations [52]. The displacement of the ester C=O stretch by about 8 cm^{-1} (from 1684 to 1692 cm^{-1}) and the observation of a weak shoulder at a low wavenumber attributable to the phenyl group stretch vibration, allow us to hypothesize the establishment of H-bonds with the apatite inorganic component. **Fig. S3** illustrates the above by giving a detailed view of the example of chlorogenic acid on biomimetic apatite in various wavenumber domains.

For complementary vibrational spectroscopy analyses, and in particular to highlight the surface features, Raman microspectroscopy analyses were carried out. Modifications of Raman features between the adsorbed state and the free molecule could be expected due to conformational changes and/or the promotion of novel interactions and/or the possible extinction of some polarized vibrators. The observation of spectral modifications could thus be a way to unveil the types of interaction existing between the molecules and the apatitic substrate. The main Raman features to be expected from a polyphenol molecule like CA have been explored more finely, both via experimental and computational viewpoints, in the literature [53]. They are especially related to the vibrational signature of the phenyl ring and the cyclohexane ring. Raman spectra were recorded on different zones of the samples. Some areas appeared whiter than others, potentially indicative of a somewhat heterogeneous distribution of the molecular species on the apatite surface, which was confirmed by spectral features closer to apatite for the darker zones and with a higher organic contribution in the whiter zones. Typical Raman spectral features observed in the whiter domains (thus containing more CA), and compared to the pure polyphenol molecule are reported in Fig. 6. These spectra tend to validate the presence of the molecule combined to the apatite phase (band at 960 cm^{-1} relating to the ν_1PO_4 vibration of apatitic phosphates), as phenyl-related and cyclohexane-related signatures appear to be present in the spectra. Yet, some modifications in terms of relative intensities and band widths can be evidenced, for example with a broadening of the 1605 cm^{-1}

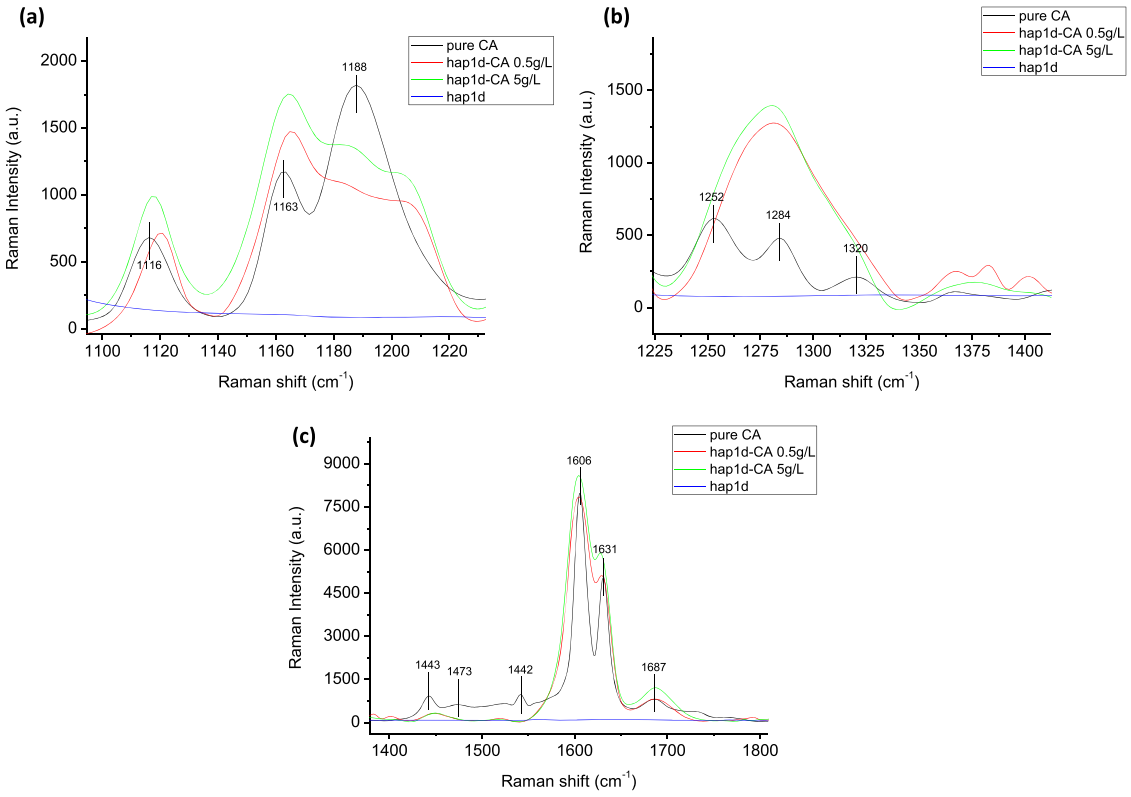

Fig. 6. Raman microspectroscopy analysis. Example of the case of chlorogenic acid (CA) in interaction with hap1d. Spectral features are given in the 1100-1230 cm^{-1} range (a), 1225-1525 cm^{-1} range (b) and 1400-1800 cm^{-1} range (c).

contribution of the phenyl ring stretching band in the hybrids compared to pure CA. Another example relates to a modification of 1250-1300 cm^{-1} domain, encompassing various contributions including δOH vibrations that seems promoting after adsorption. The domain corresponding to the C-H bending contributions of the phenyl ring at *ca.* 1188 and 1165 cm^{-1} seems to be modified after adsorption than on pure CA, with a decrease in intensity of the former and an increase of the latter. Again, these findings suggest that the phenyl ring is affected by the sorption. In contrast, it may be remarked that the vibration signature of the C=O of the carboxylic acid moiety from the cyclohexane ring does not seem to be significantly affected by the sorption process on the apatite surface, as the band at *ca.* 1686 cm^{-1} does not seem to be noticeably modified with or without CA adsorption. This may be found rather surprising at first, since it may have been guessed that the interaction between the chlorogenic acid or other biophenol acidic moiety with the apatite surface could have been made through the -COOH group. However, the exact attribution of each vibration band observed remains delicate. Indeed, as may be seen from the literature [53], each absorption can encompass different contributions from various groups in the molecule. Our findings suggest that at least some OH groups seem to be involved in the CA adsorption process.

In the case of SA (**Fig. S4**), a downshift of the bands at 820 and 1640 cm^{-1}, reasonably assigned to phenyl C-H vibration and phenyl ring deformation, respectively, is noticed in the adsorbed state, thus also indicating a modification of the chemical environment around the phenyl ring of the molecules once adsorbed. Also, a modification of the O-H band around 1450 cm^{-1} is detected, suggesting that the phenol group is altered. A decrease in intensity of the band at 1305 cm^{-1} (C-O) is however also observed as well as a downshift of the bands at 1336 cm^{-1} (COO^- stretching) and 1160 cm^{-1} (C-H bending), which could additionally imply a modification of the carboxylated end group of the molecules for SA. Again, we should highlight however the difficulty to attribute unilaterally each vibration band to one single group in the molecule. The observation of vibrational changes upon adsorption nonetheless point to a verification of the adsorbed state through some chemical interaction and not solely a mechanical mixture.

3.5. *Molecular modeling*

In order to explore further the type of interaction that may be expected between an apatitic surface and a (bio)phenolic compounds, especially taking into account the uncertainty linked to the IR/Raman band attributions, some Monte Carlo calculations were made on both chlorogenic and sinapic acids. To this day, there is no reported model for the surface of biomimetic apatites, therefore stoichiometric hydroxyapatite (HA) has been here considered as the best available model to-date. The (010) surface of bulk HA was purposely selected as it is known that bone apatite or its biomimetic synthetic analogs as those obtained in the present study are formed of nanocrystals elongated along the c-axis of the hexagonal structure.

In a subsequent stage, we then simulated the interaction between one CA molecule and the (010) apatite surface by Monte Carlo modeling, keeping in mind the presence of surrounding water molecules in the aqueous CA solution used in practice (Fig. 7a). Results suggest that the CA molecule may establish hydrogen bonds (typically considered for a bond length shorter than 3 Å) with both the apatite surface and with water molecules. Concerning the CA-surface interaction, binding seems to involve the O-H and C=O groups attached to the cyclohexane group of the CA molecule. These results thus tend to confirm the possible existence of chemical interaction – although through H-bonding – between the phenolic compound and the apatite surface, as already suggested by our FTIR and Raman spectroscopy results.

In a second stage, we added CA molecules in the Monte Carlo simulation to check whether CA-CA intermolecular bonding could overcome CA-surface interactions. As shown in our results (Fig. 7b), the CA molecule appears to retain its interaction with the apatitic surface

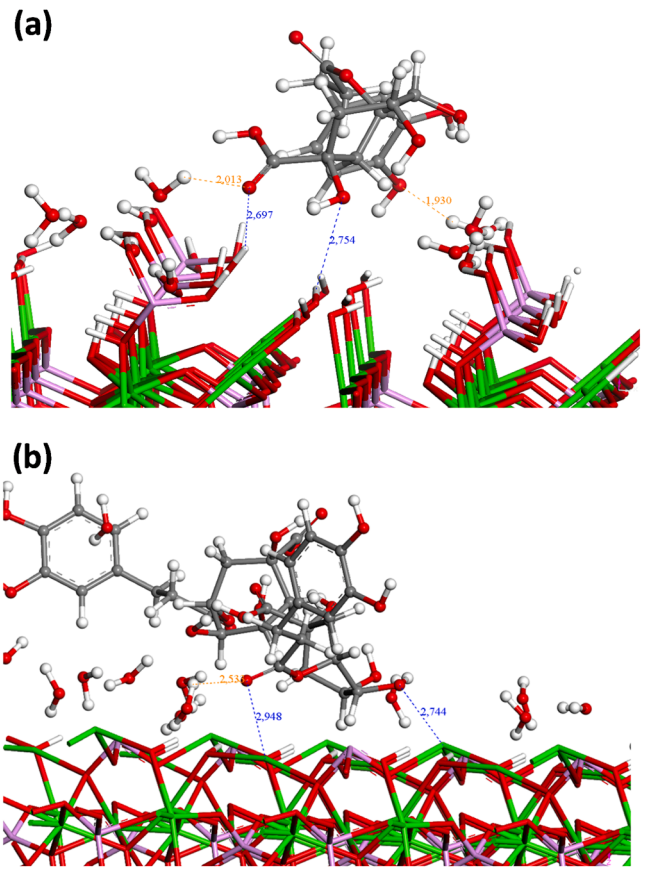

Fig. 7. (a) Monte Carlo simulation of the interaction between one CA molecule and the hydroxyapatite (010) surface and (b) similar Monte Carlo simulation with three CA molecules and water. (The atoms C, O, H, Ca, P are respectively represented in grey, red, white, green and pink).

without establishing strong bonds with an adjacent CA molecule. These findings suggest the existence of a non-negligible binding strength between the HA crystal surface and the phenolic compound. While these calculations remain preliminary, they tend to confirm our adsorption data and vibrational spectroscopy outcomes showing that the adsorption of (bio)phenolic compounds onto apatitic substrates can be seen as a relevant strategy to functionalize apatitic biomaterials with such phytotherapeutic substances. Furthermore, the comparison of the adsorption enthalpy for 1 and 3 molecules (CA or SA) shows that the synergic effect is higher for CA than for SA: the adsorption enthalpy values for 1 and 3 molecules are 122 and 138 kJ.mol^{-1} (29.2 and 32.9 kcal.mol^{-1}) for CA and 122 and 97 kJ.mol^{-1} (29.2 and 23.1 kcal.mol^{-1}) for SA respectively. This result suggests that the interactions with SA are relatively weak while that with CA are slightly stronger, in concordance with experimental data.

In the case of SA (see Fig. 8), the interaction of the molecule with the HA surface is only due to the OH group but with weaker interaction (distances are ranging around 2.3-2.5 Å as represented in Fig. 8a) than for CA. Indeed CH_3O group interacts with larger distances with HA surface. In the presence of water, the distances are relatively equivalent and no other site can be found except with water molecule (see Fig. 8b).

3.6. Retention of biophenol activity after adsorption–illustrative assessments on antioxidant activity

At this stage, it was interesting to check whether the hybrid compounds obtained exhibited indeed some antioxidant properties despite the adsorbed character of the CA and SA molecules onto biomimetic apatite substrates. In this view, DPPH is one of the most commonly used

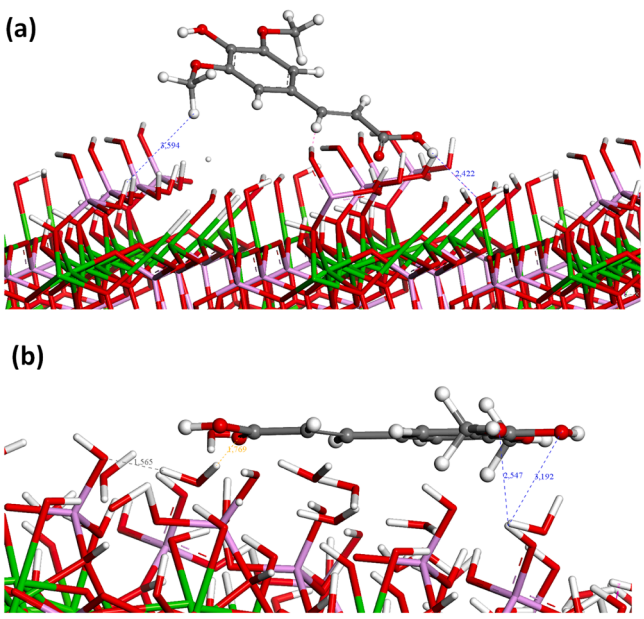

Fig. 8. (a) Monte Carlo simulation of the interaction between one SA molecule and the hydroxyapatite (010) surface and (b) similar Monte Carlo simulation in the presence of water.

radicals for assessing the antioxidant activity of foods and extracts. We thus studied here the antioxidant capacity of biomimetic apatites functionalized with antioxidant phytotherapeutics (chlorogenic or sinapic phenolic compounds) using the DPPH method. As is customary with this reactant, results are presented here in terms of percentage of DPPH free radicals trapped, as well as the corresponding IC_{50} values (Table 1). Note that these IC_{50} values thus refer, in this work, to the amount of phenolic compound included in the hybrids (in µg) per mL of solution.

Interestingly, chlorogenic acid loaded onto biomimetic apatite (initial concentration of 5 g/L) presented a major DPPH scavenging activity. This hybrid indeed demonstrated a notable antioxidant activity of 74.43± 4.13% at a concentration of 50 µg/mL, corresponding to an IC_{50} value of 18.25 ± 3.04 µg/mL. Taking into account the actual amount of CA present in the sample composition, this leads to a corrected IC_{50} value of 6.70 ± 1.11µg of CA/mL. This value can be compared to that of pure chlorogenic acid, namely 3.98 ± 0.56 µg/mL. Although a decrease in scavenging activity may be seen, the hybrid compound remains associated with a noticeable antioxidant activity as this IC_{50} value is significantly lower than 50 µg/mL which is often considered as an activity limit.

In contrast to CA, in the case of sinapic acid, the hybrid hap1d/SA (5 g/L) sample demonstrated only a limited ability to neutralize DPPH free radicals, with a percentage of inhibition not exceeding 42.36 ± 5.59% (IC_{50} greater than 50 µg/mL), while pure sinapic acid presented an IC_{50}

Table 1
Experimental % DPPH inhibition and related IC_{50} values measured in this work.

Sample	% Inhibition (50 µg of compound/mL)	IC_{50}(µg of compound/mL)
hap1d	23.26± 3.99	>50
hap1d-Ag	24.98± 7.31	>50
Chlorogenic acid (CA)	91.92± 7.05	3.98 ± 0.56
Sinapic acid (SA)	85.97± 10.08	4.15 ± 0.57
hap1d - CA 5g/L	74.43± 4.13	18.25 ± 3.04
hap1d - SA 5g/L	42.36± 5.59	>50
hap1d-Ag - CA 5g/L	57.52± 6.23	35.10 ± 9.53
hap1d-Ag - SA 5g/L	60.35± 4.83	29.42* ± 7.90

* This value remains estimative due to a larger uncertainty on the effective SA adsorbed amount.

of 4.15 ± 0.57 μg/mL. When referring only to the amount of SA associated to the hybrid, drawn from the adsorption isotherm, the corrected IC_{50} shifts to 6.31 ± 2.65 μg of SA/mL. Although only a small amount of SA was contained in the hybrid, these findings thus suggest that SA in the SA/apatite hybrid may retain a rather good specific antioxidant power (despite a decrease of activity compared to the free SA, leading to an IC_{50} of 4.15 ± 0.57 μg/ml).

It may however be noted that, for the silver-doped sample, the hap1d-Ag/CA (5g/L) and hap1d-Ag/SA (5g/L) hybrids showed a measurable ability to neutralize DPPH free radicals, with an inhibition percentage of 57.52 % for hap1d-Ag/CA (5g/L) and 60.35 % for hap1d-Ag/SA (5g/L), corresponding to IC_{50} values of 35.10 ± 9.53 and 29.42 ± 7.90 μg/mL, respectively. Thus, in both cases, the presence of Ag^+ seemed to affect negatively the antioxidant activity of CA or SA adsorbed on biomimetic apatite.

Comparison with the scarce literature data existing on this topic does not allow assessments based on absolute values of inhibition %, as experimental protocols differ. But a decrease of two-thirds of activity was evidenced by Palierse et al. [5,54] for HA-CA compared to pure CA, using a regular hydroxyapatite sample, while the present results using a biomimetic apatite substrate only reduced the inhibition % from ca. 92% for pure CA to 74% in the hybrid. Thus, it seems that opting for a more reactive biomimetic apatite adsorbate promotes the antioxidant activity of polyphenols like chlorogenic acid, and could be considered appealing in further studies.

4. Overview

Plant-derived biophenolic compounds exhibit a large variety of advantageous properties such as antibacterial, antioxidant, etc. These properties are very appealing in the field of bone repair as in orthopedic and maxillofacial surgeries. It thus appears very promising to fabricate biomaterials for which the bioactivity can be promoted thanks to an adsorption of such biophenolic compounds. In addition, in this work we have selected a substrate for this adsorption that is itself very bioactive, namely biomimetic apatites. It thus was relevant to try and obtain hybrid biomaterials (in view of bone substitute applications) combining bone-like apatite and adsorbed biophenolic compounds (in view of added biological properties such as antimicrobial, antioxidant, etc.). While several attempts to adjoin antibacterial features to apatites have been tried and reported with a series of drugs like antibiotics, etc., it is interesting to explore other properties in relation to apatites, such as antioxidant ones. Thus, the originality of this study may be summarized by the following points:

- For the first time, CA and SA adsorption on bone-like biomimetic apatite mimicking the actual composition and structure of bone mineral has been investigated;
- A dual experimental and computational study is provided to explore the type of interaction that can be expected between such biophenolic compounds of interest and an apatite substrate;
- For the first time, co-functionalization with both Ag^+ antimicrobial ions and biophenolic (plant-derived) molecules compounds has been investigated, and hybrids have been successfully obtained;
- We have shown that the “fully bio-inspired” hybrid compounds generated in this work could retain an antioxidant character after adsorption of some phenolic compound, thus evidencing the relevance of the study in the field of bioactive bone substitutes.

Regarding apatitic substrates, the vast literature on this matter has shown general principles. Among those, it may be retained that smaller molecules (like CA or SA for example) general have higher propensity to adsorb quantitatively onto the apatitic substrate than large macromolecules such as proteins or DNA. The adsorption affinity is however also dictated, to some extent, by the exposure of charged end-groups that may more energetically interact with the apatite surface. To be even more precise, negatively-charged groups like carboxylates, phosphates or phosphonates, were shown to exert the highest interaction with calcium ions from the surface of apatite (nano)crystals. Although the adsorption of other organic moieties may occur, to some extent, after implantation of implants like apatite-based ones, the pre-adsorption of small negatively-charged molecules like CA or SA is expected to be somehow predominant. This is thus a rather favorable scenario for the hybrid compounds that have been prepared in this work. This now opens the way to future more focused studies using these compounds toward clinical use, which will require additional experiments such as *in vitro* tests and competitive adsorption experiments if judged pertinent. It may however be mentioned that the release of CA or SA once implanted could be advantageous to exert a local bioactivity (e.g. antioxidant, antibacterial, anti-inflammatory…). This is, in any case, what is expected to happen as bone-like apatites are resorbable and will help the bone repair process while releasing the attached adsorbed molecules, if any.

5. Conclusion

In this study, we examined the interaction between nanocrystalline biomimetic apatites (doped or non-doped with antibacterial silver ions), close to the mineral part of natural bone, and phytotherapeutic molecules, namely chlorogenic acid (CA) and sinapic acid (SA). The obtained hybrids were characterized by complementary techniques including FTIR, Raman and XRD. Kinetics and isotherms of adsorption were determined in the best conditions possible taking into account the relative instability of these molecules. Care was in particular taken to manipulate the compounds in the dark as much as possible prior to analyses. Our results suggest that the sorption of such plant-derived biophenolic compounds onto biomimetic apatites can be considered as quantitative and thus to be a promising way to combine (poly)phenolic phytotherapeutic molecules and bone-like ceramics to yield bioactive bone substitutes with advanced properties including antioxidant ones. The latter were indeed followed in the prepared hybrids. Experimental data, especially based on Raman microspectroscopy, along with computational simulations through Monte-Carlo calculations concurred to show the possible chemical interaction between such molecular species and an apatite surface. This work suggests that bone-like biomimetic apatites can adsorb larger amounts of such biophenolic substances than more regular apatitic substrates form the literature, including nanocrystalline but not biomimetic ones, and may favor a new pathway to innovation in the field of bioactive ceramics.

CRediT authorship contribution statement

Omar Baklouti: Writing – review & editing, Writing – original draft, Investigation, Formal analysis, Data curation, Conceptualization. **Olivier Marsan:** Writing – review & editing, Investigation, Formal analysis, Data curation. **Fabrice Salles:** Writing – review & editing, Investigation, Formal analysis, Data curation. **Jalloul Bouajila:** Writing – review & editing, Investigation, Formal analysis, Data curation. **Hafed El-Feki:** Writing – review & editing, Supervision, Investigation, Funding acquisition, Conceptualization. **Christophe Drouet:** Writing – review & editing, Writing – original draft, Supervision, Investigation, Formal analysis, Data curation, Conceptualization.

Declaration of competing interest

The authors do not have any disclosure to mention.

Acknowledgements

O. Baklouti thanks the University of Sfax for funding his mobility to France.

Supplementary materials

Supplementary material associated with this article can be found, in the online version, at doi:10.1016/j.mtla.2024.102271.

References

[1] M. Catauro, et al., Antibacterial and cytotoxic silica-polycaprolactone-chlorogenic acid hybrids by sol–gel route, Molecules 28 (2023), https://doi.org/10.3390/molecules28083486.
[2] F. Natella, et al., Benzoic and cinnamic acid derivatives as antioxidants: structure-activity relation, J. Agric. Food Chem. 47 (4) (1999) 1453–1459.
[3] S. D'Angelo, et al., Pro-oxidant and pro-apoptotic activity of polyphenol extract from Annurca apple and its underlying mechanisms in human breast cancer cells, Int. J. Oncol. 51 (3) (2017) 939–948.
[4] A.J. León-González, C. Auger, V.B. Schini-Kerth, Pro-oxidant activity of polyphenols and its implication on cancer chemoprevention and chemotherapy, Biochem. Pharmacol. 98 (3) (2015) 371–380.
[5] E. Palierse, et al., Synthesis of hybrid polyphenol/hydroxyapatite nanomaterials with anti-radical properties, Nanomaterials 12 (20) (2022) (Basel).
[6] M. Mzid, et al., Chemical composition, phytochemical constituents, antioxidant and anti-inflammatory activities of Urtica urens L. leaves, Arch. Physiol. Biochem. 123 (2) (2017) 93–104.
[7] J. Santana-Gálvez, L. Cisneros-Zevallos, D.A. Jacobo-Velázquez, Chlorogenic acid: recent advances on its dual role as a food additive and a nutraceutical against metabolic syndrome, Molecules 22 (3) (2017).
[8] M. Naveed, et al., Chlorogenic acid (CGA): a pharmacological review and call for further research, Biomed. Pharmacother. 97 (2018) 67–74.
[9] N. Liang, D.D. Kitts, Role of chlorogenic acids in controlling oxidative and inflammatory stress conditions, Nutrients 8 (1) (2015).
[10] K.H. Lee, et al., Impact of chlorogenic acid on modulation of significant genes in dermal fibroblasts and epidermal keratinocytes, Biochem. Biophys. Res. Commun. 583 (2021) 22–28.
[11] S. Feng, et al., Application of chlorogenic acid as a substitute for antibiotics in multidrug-resistant Escherichia coli-induced mastitis, Int. Immunopharmacol. 114 (2023) 109536.
[12] M.F. Lemos, et al., Chlorogenic acid and caffeine contents and anti-inflammatory and antioxidant activities of green beans of conilon and arabica coffees harvested with different degrees of maturation, J. Saudi Chem. Soc. 26 (3) (2022) 101467.
[13] X. Wang, et al., Chlorogenic acid inhibits proliferation and induces apoptosis in A498 human kidney cancer cells via inactivating PI3K/Akt/mTOR signalling pathway, J. Pharm. Pharmacol. 71 (7) (2019) 1100–1109.
[14] M. Su, et al., The antibacterial activity and mechanism of chlorogenic acid against foodborne pathogen Pseudomonas aeruginosa, Foodborne Pathog. Dis. 16 (12) (2019) 823–830.
[15] L. Wang, et al., Effects of chlorogenic acid on antimicrobial, antivirulence, and anti-quorum sensing of carbapenem-resistant Klebsiella pneumoniae, Front. Microbiol. 13 (2022).
[16] Y. Zhao, et al., Antihypertensive effects and mechanisms of chlorogenic acids, Hypertens. Res. 35 (4) (2012) 370–374.
[17] S. Meng, et al., Roles of chlorogenic Acid on regulating glucose and lipids metabolism: a review, Evid. Based Complement. Altern. Med. 2013 (2013) 801457.
[18] K.W. Ong, A. Hsu, B.K. Tan, Anti-diabetic and anti-lipidemic effects of chlorogenic acid are mediated by ampk activation, Biochem. Pharmacol. 85 (9) (2013) 1341–1351.
[19] R. Sousa, et al., Is asymptomatic bacteriuria a risk factor for prosthetic joint infection? Clin. Infect. Dis. 59 (1) (2014) 41–47.
[20] L. Fu, W. Lu, X. Zhou, Phenolic compounds and *in vitro* antibacterial and antioxidant activities of three tropic fruits: persimmon, guava, and sweetsop, Biomed. Res. Int. 2016 (2016) 4287461.
[21] M.T. Ayseli, Y.İ. Ayseli, Flavors of the future: health benefits of flavor precursors and volatile compounds in plant foods, Trends Food Sci. Technol. 48 (2016) 69–77.
[22] M.H. Farzaei, M. Abdollahi, R. Rahimi, Role of dietary polyphenols in the management of peptic ulcer, World J. Gastroenterol. 21 (21) (2015) 6499–6517.
[23] A. Karunanidhi, et al., *In vitro* antibacterial and antibiofilm activities of chlorogenic acid against clinical isolates of Stenotrophomonas maltophilia including the trimethoprim/sulfamethoxazole resistant strain, Biomed. Res. Int. 2013 (2013) 392058.
[24] E. Bajko, et al., 5-O-Caffeoylquinic acid: a spectroscopic study and biological screening for antimicrobial activity, LWT Food Sci. Technol. 65 (2016) 471–479.
[25] Y.C. Fiamegos, et al., Antimicrobial and efflux pump inhibitory activity of caffeoylquinic acids from Artemisia absinthium against gram-positive pathogenic bacteria, PLoS ONE 6 (4) (2011) e18127.
[26] M. Stauder, et al., Antiadhesion and antibiofilm activities of high molecular weight coffee components against Streptococcus mutans, J. Agric. Food Chem. 58 (22) (2010) 11662–11666.
[27] E.A. Hudson, et al., Characterization of potentially chemopreventive phenols in extracts of brown rice that inhibit the growth of human breast and colon cancer cells, Cancer Epidemiol. Biomark. Prev. 9 (11) (2000) 1163–1170.
[28] N. Nićiforović, H. Abramovič, Sinapic acid and its derivatives: natural sources and bioactivity, Compr. Rev. Food Sci. Food Saf. 13 (1) (2014) 34–51.
[29] H. Nowak, et al., Antioxidative and bactericidal properties of phenolic compounds in rapeseeds, Lipid /Fett 94 (4) (1992) 149–152.
[30] L. Quinn, et al., An *in vitro* study determining the anti-inflammatory activities of sinapinic acid-containing extracts generated from Irish rapeseed meal, Med. Res. Arch. 8 (10) (2020), https://doi.org/10.18103/mra.v8i10.2225. VolNoVol.8 Issue 10 October 20202020.
[31] K.J. Yun, et al., Anti-inflammatory effects of sinapic acid through the suppression of inducible nitric oxide synthase, cyclooxygase-2, and proinflammatory cytokines expressions via nuclear factor-kappaB inactivation, J. Agric. Food Chem. 56 (21) (2008) 10265–10272.
[32] W.Y. Li, et al., Sinapic acid attenuates chronic DSS-induced intestinal fibrosis in C57BL/6J mice by modulating NLRP3 inflammasome activation and the autophagy pathway, ACS Omega 9 (1) (2024) 1230–1241.
[33] S. Fu, et al., Preparation and characterisation of chlorogenic acid-gelatin: a type of biologically active film for coating preservation, Food Chem. 221 (2017) 657–663.
[34] Y. Zou, et al., Electrospun chitosan/polycaprolactone nanofibers containing chlorogenic acid-loaded halloysite nanotube for active food packaging, Carbohydr. Polym. 247 (2020) 116711.
[35] B. Niu, et al., Co-encapsulation of chlorogenic acid and cinnamaldehyde essential oil in Pickering emulsion stablized by chitosan nanoparticles, Food Chem. X 14 (2022) 100312.
[36] M. Cazzola, et al., Bioactive glass coupling with natural polyphenols: surface modification, bioactivity and anti-oxidant ability, Appl. Surf. Sci. 367 (2016) 237–248.
[37] M. Dziadek, et al., PCL and PCL/bioactive glass biomaterials as carriers for biologically active polyphenolic compounds: comprehensive physicochemical and biological evaluation, Bioact. Mater. 6 (6) (2021) 1811–1826.
[38] S. Palaniraj, R. Murugesan, S. Narayan, Chlorogenic acid- loaded calcium phosphate chitosan nanogel as biofilm degradative materials, Int. J. Biochem. Cell Biol. 114 (2019) 105566.
[39] S. Sarda, et al., Interaction of folic acid with nanocrystalline apatites and extension to methotrexate (Antifolate) in view of anticancer applications, Langmuir 34 (40) (2018) 12036–12048.
[40] C.G. Weber, et al., Enzyme-functionalized biomimetic apatites: concept and perspectives in view of innovative medical approaches, J. Mater. Sci. Mater. Med. 25 (3) (2014) 595–606.
[41] M.I. Kay, R.A. Young, A.S. Posner, Crystal structure of hydroxyapatite, Nature 204 (1964) 1050–1052.
[42] J.L.F. Abascal, C. Vega, A general purpose model for the condensed phases of water: TIP4P/2005, J. Chem. Phys. 123 (23) (2005) 234505.
[43] M.M. Saoudi, J. Bouajila, K. Alouani, Phenolic compounds of Rumex roseus L. extracts and their effect as antioxidant and cytotoxic activities, Biomed. Res. Int. 2021 (2021) 2029507.
[44] C. Drouet, et al., Nanocrystalline apatites: the fundamental role of water, Am. Mineral. 103 (4) (2018) 550–564.
[45] N. Vandecandelaere, C. Rey, C. Drouet, Biomimetic apatite-based biomaterials: on the critical impact of synthesis and post-synthesis parameters, J. Mater. Sci. Mater. Med. 23 (11) (2012) 2593–2606.
[46] I.D. Ana, et al., Safe-by-design antibacterial peroxide-substituted biomimetic apatites: proof of concept in tropical dentistry, J. Funct. Biomater. 13 (2022), https://doi.org/10.3390/jfb13030144.
[47] S. Cazalbou, G. Bertrand, C. Drouet, Tetracycline-loaded biomimetic apatite: an adsorption study, J. Phys. Chem. B (2015).
[48] K. Hammami, et al., Adsorption of nucleotides on biomimetic apatite: the case of adenosine 5 ' monophosphate (AMP), Appl. Surf. Sci. 353 (2015) 165–172.
[49] Palierse, E., et al., Synthesis of hybrid polyphenol/hydroxyapatite nanomaterials: adsorption vs. *in situ* incorporation. ChemRxiv, 2021. 2021: p. 31 pages.
[50] S. Mishra, et al., Vibrational spectroscopy and density functional theory analysis of 3-O-caffeoylquinic acid, Spectrochim. Acta A Mol. Biomol. Spectrosc. 104 (2013) 358–367.
[51] M. Catauro, S. Pacifico, Synthesis of bioactive chlorogenic acid-silica hybrid materials via the sol–gel route and evaluation of their biocompatibility, Materials 10 (2017), https://doi.org/10.3390/ma10070840.
[52] G. Shi, et al., Yeast-cell-based microencapsulation of chlorogenic acid as a water-soluble antioxidant, J. Food Eng. 80 (4) (2007) 1060–1067.
[53] P.J. Eravuchira, et al., Raman spectroscopic characterization of different regioisomers of monoacyl and diacyl chlorogenic acid, Vib. Spectrosc. 61 (2012) 10–16.
[54] Palierse, E., et al. Synthesis of hybrid polyphenol/hydroxyapatite nanomaterials: adsorption vs. *in situ* incorporation. ChemRxiv, 2021. 2021, 31 pages doi: 10.26434/chemrxiv-2021-39frr.